LUND UNIVERSITY

Measurements of the optical properties of tissue in conjunction with photodynamic therapy

Nilsson, A. M. K.; Berg, R.; Andersson-Engels, Stefan

[Link to publication](#)

Measurements of the optical properties of tissue in conjunction with photodynamic therapy

Annika M. K. Nilsson, Roger Berg, and Stefan Andersson-Engels

A simple optical dosimeter was used to measure the light intensity in rat liver and muscle *in vivo* with fibers positioned at different depths to investigate whether the light penetration changed during photodynamic therapy (PDT). The results were then correlated with measurements of the three optical-interaction coefficients μ_s, μ_a, and g for wavelengths in the range 500–800 nm for PDT-treated and nontreated rat liver and muscle tissue *in vitro*. A distinct increase in the absorption coefficient was seen immediately after treatment, in agreement with the decreasing light intensity observed during the treatment, as measured with the optical dosimeter. The collimated transmittance was measured with a narrow-beam setup, and an optical integrating sphere was used to measure the diffuse reflectance and total transmittance of the samples. The corresponding optical properties were obtained by spline interpolation of Monte Carlo-simulated data. To ensure that the measured values were correct, we performed calibration measurements with suspensions of polystyrene microspheres and ink.

Key words: Light penetration, optical properties, photodynamic therapy, tissue optics.

1. Introduction

Photodynamic therapy (PDT) is a method of tumor treatment employing photosensitizers and laser light. The treatment modality is based on the administration of a photosensitizer to the patient. The photosensitizer is, after a while, selectively accumulated in malignant tissue, and the tumor area is then irradiated with red laser light. The light excites the photosensitizer, and the excitation energy is transferred to the surrounding oxygen molecules, which causes tissue oxidation and destruction of the microcirculation in the tumor.[1,2] In treatment planning, it is essential to know how the light is transported within the tissue to be able to optimize the results of the treatment. If the optical properties of the tissue are known, the light dose delivered to the tissue can be calculated. Any changes in these optical parameters, and thus in the light penetration, must therefore be carefully controlled. The aim of this study was to ascertain whether the optical properties of tissue change during PDT.

When light interacts with any kind of tissue, it is either absorbed or scattered, in various proportions, depending on the optical properties of the tissue. To model this interaction, one uses transport theory. This theory quantifies the tissue optical properties in terms of the absorption coefficient μ_a, the scattering coefficient μ_s, and the anisotropy factor g. The absorption and scattering coefficients describe the probability of photon absorption and scattering per unit path length. The anisotropy coefficient, which is the mean value of the cosine of the scattering angle, describes at what angles the photons are scattered. The attenuation coefficient μ_t is given by the sum of μ_s and μ_a. The optical thickness τ is defined as the attenuation coefficient multiplied by the physical thickness of the sample, d.

$$\mu_t = \mu_s + \mu_a, \tag{1a}$$

$$\tau = d\mu_t. \tag{1b}$$

A wide range of experimental techniques, theoretical models, approximations, calibration routines, tissue-preparation techniques, etc., are used to obtain these optical coefficients.[3] The absorption coefficient μ_a and the reduced-scattering coefficient μ_s' $[= \mu_s(1 - g)]$ can be determined with time-resolved or spatially resolved measurements of diffusely scattered light from the tissue through the use of the diffusion approximation.[4,5] One of the major advantages of this method is the possibility to measure independently the two optical constants μ_s' and μ_a not only for tissue samples *in vitro* but also *in vivo*.

However, this approximation is valid only when the light is diffusely scattered, which means that rather thick, highly scattering specimens are needed. To obtain a complete set of the optical properties, g, μ_s, and μ_a, an integrating-sphere method is usually used. Several different models and approximations of the radiance transport equation can be used to correlate the macroscopic quantities measured to the microscopic optical constants.[6,7] Apart from the Kubelka–Munk theory[8] and the diffusion theory,[9] both of which assume a diffuse photon fluence, there is the inverse adding–doubling method,[10,11] which takes into account anisotropic scattering. Light propagation can also be modeled by simulation of photon random walks through the use of Monte Carlo simulations.[12] Monte Carlo simulation is considered to be the most accurate and most flexible method, as it can predict the light fluence for a wide range of optical parameters and for most boundary conditions.

In this study, we used an integrating-sphere technique combined with Monte Carlo simulations to determine and compare the optical properties of tissue before and after PDT, with the aim of investigating whether the treatment induced any changes in these properties. Such changes would alter the light penetration and would be of importance in treatment dosimetry.

2. Materials and Methods

A. Experimental Layout

Two different experiments were performed. To obtain an initial indication of the changes in the optical properties of tissue in conjunction with photodynamic therapy, we measured the light penetration *in vivo* with a simple light dosimeter during PDT. This is further described in Section 2.C. The other experiment involved the PDT of photosensitized or, for control, nonphotosensitized tissue. Two different photosensitizers were used. The PDT was followed by measurements of the optical properties of resected tissue samples. Before each treatment in this experiment, the abdominal wall of each rat was cut open, and laser-induced fluorescence of the median liver lobe was registered. An area of this lobe was then treated with PDT, leaving an untreated area of almost the same size. Following this treatment, the median liver lobe was resected, and the optical properties were measured with the integrating-sphere setup. The measurements lasted approximately 30 min. During this time the abdominal wall was temporarily closed and the skin covering the femoral muscle was cut open. The fluorescence of the muscle tissue was measured and an area of muscle was treated with PDT. After the treatment, a superficial muscle specimen that included both treated and untreated regions was resected. During the integrating-sphere measurements of the two muscle areas, the same procedure, including PDT, fluorescence recordings, tissue preparation, and integrating-sphere measurements, was commenced for the left-lateral liver lobe. After the last measurement the animal was sacrificed.

B. Animal Preparation and Operating Procedures

Seventeen Spraque-Dawley rats with weights ranging 275–375 g were used in the experiments. The animals were divided into four groups. In group I (two animals) the light-fluence rate in the tissue was measured with a simple dosimeter during two sequential PDT irradiations of the median and left-lateral liver lobes. The animals received 30 mg/kg body weight (b.w.) δ-amino levulinic acid (ALA) i.v. 30 min before illumination. For the other three groups, the optical coefficients of the treated and untreated tissues were measured with the optical-integrating-sphere setup. Group II (nine animals) received 30 mg/kg b.w. ALA i.v. 30 min, 1.5 h, and 2.5 h prior to the treatment of the median liver lobe, the femoral muscle, and the left-lateral liver lobe. Group III (three animals) received 15 mg/kg b.w. Photofrin i.v. 3, 4, and 5 h before the treatment of the median liver lobe, the femoral muscle, and the left-lateral liver lobe. Finally, for group IV (three control animals) the same procedure was repeated without any photosensitizer administered. All animals were permitted free access to water and food (ordinary pellet diet) prior to the experiment.

The animals were anaesthetized with 5% chloral hydrate intraperitoneally. Twenty milliliters of Ringer's–glucose solution were injected intraoperatively into the subcutaneous tissue of the animal's back for volume replacement. All operations were performed under clean conditions. The abdomen was cut open through a midline incision, and the liver lobes were exposed. The tissue samples were taken from two of the four liver lobes, the left-lateral and the median lobes, and from the femoral muscle for all groups except group I. The samples were resected immediately after the treatment to prevent any posttreatment changes. No bleeding was observed in any of these resections. A 1-mm-thick slice of the superficial tissue, including a treated as well as a nontreated area, was removed and placed between two glass slides with 1.0-mm glass spacers in between. Measurements of the optical properties for wavelengths between 500 and 800 nm of both the treated and the nontreated areas commenced less than 10 min after the PDT irradiation.

C. Measurements of the Light Penetration

To investigate variations in the light penetration *in vivo* during treatment, we positioned aluminum-jacketed optical fibers with a diameter of 300 μm at two different depths, approximately 1 and 3 mm, in the liver tissue, as shown in Fig. 1. The light-fluence rate at these depths was measured throughout the PDT irradiations. The measured fluence rate in the tissue was divided by the output laser intensity to compensate for laser-intensity fluctuations. Two liver lobes in both rats from group I were irradiated and observed in this way. The treatment was complete after approximately 15 min. After the treatment, the laser was switched on for approximately 15 s every fifth minute, to investigate any posttreat-
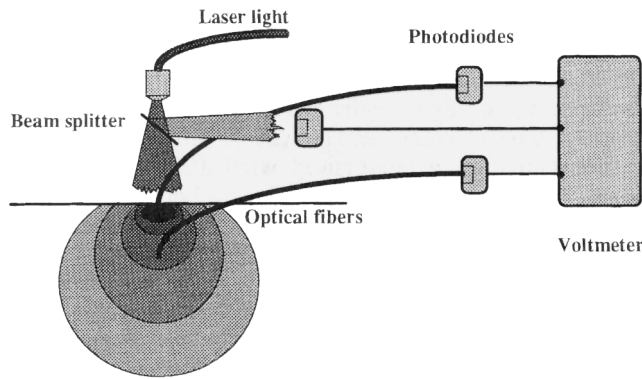
Fig. 1. Schematic outline of the setup used to measure the light-fluence rate at two depths during PDT. The optical fibers to detect the laser light were placed at depths of 1 and 3 mm in the tissue sample depicted at the lower left corner in the figure. The collected light was measured with photodiodes connected to a voltmeter. A beam splitter was placed in the laser beam to permit compensation for laser-intensity fluctuations by partly deflecting the beam to a photodiode connected to the voltmeter.

ment changes in the optical properties of the tissue. This procedure was repeated three to six times after the completed treatment, i.e., for 15–30 min.

D. Laser-Induced Fluorescence

Fluorescence measurements were performed with an optical multichannel analyzer system, described in detail in Ref. 13, to measure the presence of photosensitizers. Briefly, an N_2-laser-pumped dye laser at 405 nm was used for excitation. This excitation light was guided through an optical fiber. The clear-cut distal fiber end was in direct contact with the tissue being examined. Part of the emitted fluorescence light from the irradiated sample area was collected through the same optical fiber, guided back to the instrument, and detected with an image-intensified diode-array detector connected to a polychromator. Such spectra were taken from all investigated areas before PDT irradiation.

To be able to compare the fluorescence measurements from different tissue specimens, we evaluated a dimensionless fluorescence ratio. The photosensitizer-related fluorescence intensity at 635 nm (ALA-treated rats) or 630 nm (Photofrin-treated rats) was divided by the tissue autofluorescence intensity around 500 nm. Forming this dimensionless fluorescence intensity ratio eliminated the influence of source fluctuations. This fluorescence ratio is related to the amount of photosensitizer in the tissue.

E. Illumination

For each animal, three circular regions with diameters of 1.5 cm were irradiated with a light energy density of 60 J/cm² at 635 nm (ALA-treated rats) or 630 nm (Photofrin-treated rats): two regions on normal liver lobes and one on normal femoral muscle. During the irradiation, the average power density was kept well below 100 mW/cm² to avoid any hyperthermic effects in the tissue. As the light source, a

dye laser pumped with an intracavity frequency-doubled Nd:YAG laser, Q switched at a pulse-repetition rate of 4 kHz, was used (Technomed International Multilase Dye 600).

F. Measurements of Optical Properties

A setup with an optical integrating sphere, shown in Fig. 2, was used to determine the optical properties of the tissue samples. For these measurements, a 75-W high-pressure Xe lamp connected to a 12-cm monochromator with a 1200-line/mm grating was used as a light source. An IR filter was placed in front of the monochromator to prevent IR light from entering and damaging it. This arrangement yielded a 5-nm-bandwidth source. A chopper connected to a lock-in amplifier ensured that no nonmodulated background light was registered. The light was focused into an optical fiber with a core diameter of 200 μm and a numerical aperture of 0.22. At the other end of the fiber, the light beam was collimated with a 2.5-cm-focal-length lens and an aperture stop, resulting in a beam diameter of 5 mm at both sample positions of the sphere.

The totally transmitted and reflected light was measured with a photodiode mounted on an optical integrating sphere. The signal was amplified with a lock-in amplifier (Stanford Research Systems, model SR830), and the measured values were fed to a computer (not shown). The sphere (Oriel) was 20.3 cm in diameter, and its inner surface was covered with barium sulfate. The highly reflecting inner surface allowed light entering the sphere from any direction to be detected by the photodiode with the same efficiency. The two beam ports of the sphere that were used were opposite one another, and both had diameters of 2.5 cm. A baffle mounted inside the sphere blocked the specularly reflected light from the tissue sample at the exit port from reaching the detector. The reflectance and transmit-
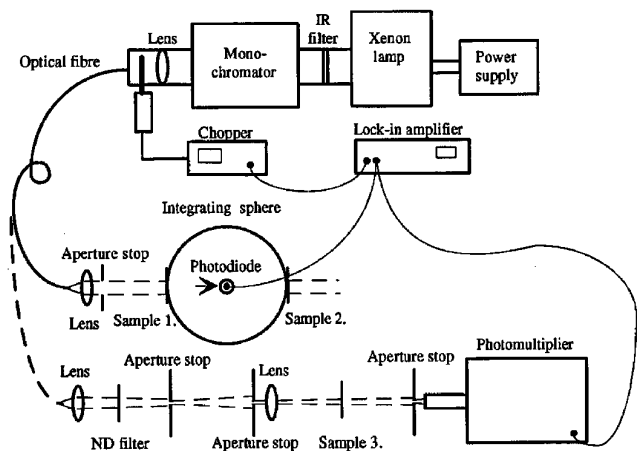

Fig. 2. Setup for the integrating-sphere and collimated-beam measurements of tissue optical properties. The total transmittance, the diffuse reflectance, and the collimated transmittance were measured by our placing the sample at positions 1, 2, and 3, respectively.

tance were then obtained by

$$T = I_T/I_{\text{ref}}, \tag{2}$$

$$R = R_{\text{BS}}(I_R/I_{\text{ref}}), \tag{3}$$

where I_R is the measured intensity at the photodiode when the light beam enters the first port and the exit port is covered by the tissue sample. I_T is the intensity measured when the entry port is covered by the tissue slab and a highly reflecting barium sulfate plug is in the exit port. The reference intensity I_{ref} is measured when the light beam enters the entry port and the barium sulfate plug is in the exit port. R_{BS} is the calibrated reflectance of this barium sulfate plug.

To measure the directly transmitted light through the tissue sample, a narrow-beam experiment was conducted with a spatially well-filtered light beam and a lock-in technique with a photomultiplier tube (PMT; Hammamatsu R928) as the detector. (See the dashed-line optical-fiber path in Fig. 2.) Spatial filtering was accomplished with the 200-μm core-diameter optical fiber when an aperture stop with a diameter of 1 mm was placed at the beam focus in between two, 20.3-cm-focal-length lenses. A distance of 60 cm was used between the sample and the 1.5-mm-diameter detector aperture. Schott neutral density (ND) filters were placed in front of the PMT during I_0 measurements to minimize any effects of nonlinearities in the detector. I_0 was the intensity measured with a water-filled reference cuvette at the sample position. The attenuation coefficient is then given by

$$\mu_t = -\ln[(I/I_0)(T_{\text{ND}})]/d, \tag{4}$$

where I is the intensity measured for a tissue sample between two glass microscope slides, T_{ND} is the transmittance of the neutral-density-filter set used for the I_0 measurement, and d is the thickness of the sample, here 1 mm.

The measured quantities R, T, and μ_t were linked to the optical-interaction coefficients μ_s, μ_a, and g by a Monte Carlo-simulation program (described in detail in Ref. 14) run on a DECpc αXP 150 computer (Digital Equipment Corporation). Monte Carlo simulations can be described as a random walk of photons. Each step of the photon packet is randomized, yielding an average distance between the interaction sites of $(\mu_s + \mu_a)^{-1}$. In each step, the photon-packet weighting is decreased by a factor of $\mu_a/(\mu_s + \mu_a)$, as a result of absorption, until it falls below a threshold level and the photon packet is terminated. If it is permitted to continue its walk, the deflection angle is randomized. The probability distribution used for the cosine of the deflection angle was the Henyey–Greenstein function:

$$P(\cos\theta) = (1 - g^2)/[2(1 + g^2 - 2g\cos\theta)^{3/2}], \tag{5}$$

which has been found to fit light scattering in biological media well.[15] If, during the walk, the photon packet leaves the medium at its front or rear surface, the photon weight will contribute to the macroscopic quantities R or T, respectively.

Besides the optical-interaction coefficients, the input parameter for the Monte Carlo simulations is the geometry of the material. In our case, a 1-mm-thick tissue sample with a refractive index of $n = 1.4$ was used between two 1-mm-thick glass slides ($n = 1.52$). Simulations were performed with 100,000 photons for all combinations of 17 values of g between 0.6 and 0.99, 10 values of μ_s (5–95 mm^{-1}), and 10 values of μ_a (0.02–5 mm^{-1}). The resulting R and T pairs were arranged in a table for each of the 17 factors of g, and a two-dimensional spline interpolation was performed for every measured R and T pair. Possible μ_s and μ_a coefficients were then listed and summarized to μ_t coefficients for all the g factors. Three one-dimensional spline interpolations, with the measured value of μ_t as the input parameter, were then needed to obtain a complete set of the optical-interaction coefficients.

G. Calibration of the Integrating-Sphere Setup

Suspensions of uniform microspheres (Duke Scientific Corporation) and ink were used for the calibration measurements. Two batches of polystyrene spheres with diameters of 0.806 and 1.53 μm were used. They were diluted in distilled water to concentrations yielding scattering coefficients and g factors in the range of those for liver and muscle tissue. Ink was added to the suspensions as an absorber in concentrations corresponding to the absorption coefficients of liver and muscle tissue. The scattering coefficient and anisotropy factor of the spheres were derived from Mie-scattering calculations,[16,17] and the absorption coefficient of the ink was measured with a spectrophotometer for a range of dilutions. The polystyrene spheres were considered not to have any absorption and the ink to have no scattering. The g factors and the scattering coefficients of the suspensions were therefore assumed to be determined by the polystyrene spheres, and the ink concentration gave the absorption coefficient of the suspension. The narrow-beam and integrating-sphere measurements were performed with the suspension in a glass cuvette that had a total thickness of 3 mm, i.e., two 1-mm-thick glass layers with a 1-mm-thick suspension layer in between. Five measurements were performed for each polystyrene sphere–ink suspension at seven wavelengths between 500 and 800 nm.

3. Results

A. Light Penetration during PDT

Figure 3 shows an example of the normalized light-fluence rate in the tissue as a function of time. In these measurements, the light was collected by an optical fiber and the measured fluence rate was divided by the direct laser-power output. PDT was administered during the first 15 minutes, and a reduction in the light intensity can be seen. Every fifth minute after the treatment, the laser light was turned on for approximately 15 s to ascertain whether there were any changes in the light penetration. The light intensity was found to decrease, but one of
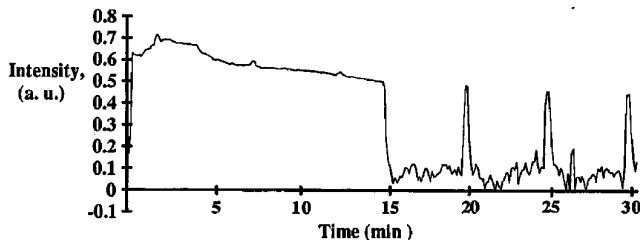
Fig. 3. Plot of the light-fluence rate as measured with the setup shown in Fig. 1: The light fluence, collected by an optical-fiber tip at a tissue depth of 1-mm, is plotted versus time during (from 0–15 min) and after (from 15 min onward) PDT. The peaks result from switching the light on for a short while every fifth minute after the completed treatment.

the measurements showed a slight recovery of the light penetration after approximately 5–10 min. The same curve form was registered by the second fiber at the depth of approximately 3 mm in the tissue. This result reduces the probability that the observed effect is due to any local events around the fiber, for example, blood coagulation caused by capillary rupture when the fiber is inserted.

B. Calibration of the Integrating-Sphere Setup

The calibration measurements performed with the polystyrene-sphere suspensions showed good agreement with the Mie-scattering computations and with the spectrophotometer measurements. Figure 4

shows a comparison between the measured optical properties and the reference values at 650 nm. Similar results were obtained for the other six measured wavelengths between 500 and 800 nm. The scattering coefficient exhibited particularly good agreement. The measured anisotropy factor was consistently somewhat low, but by only 1–3%. The absorption coefficients had rather high standard deviations, as have been found by other authors,[11] and these are ascribed to the differences in magnitude between the absorption and scattering coefficients for the samples studied. The absorption coefficients derived from the absorbance measurements of ink only were within the limits of the standard deviations of the absorption coefficients measured with the integrating-sphere technique.

C. Laser-Induced Fluorescence

The fluorescence measurements were performed immediately prior to the treatment. As can be seen in Fig. 5, the fluorescence ratio, which is related to the amount of photosensitizer, was on average 5.2 for the median liver lobes that were treated 30 min after the ALA injection and approximately 3 times higher, 15.1, for the left-lateral liver lobes that were treated 2.5 h after the ALA injection. The fluorescence ratios for the Photofrin-injected rats were considerably higher but showed no differences between the two liver lobes, i.e., on average 30.5 for the first liver lobe

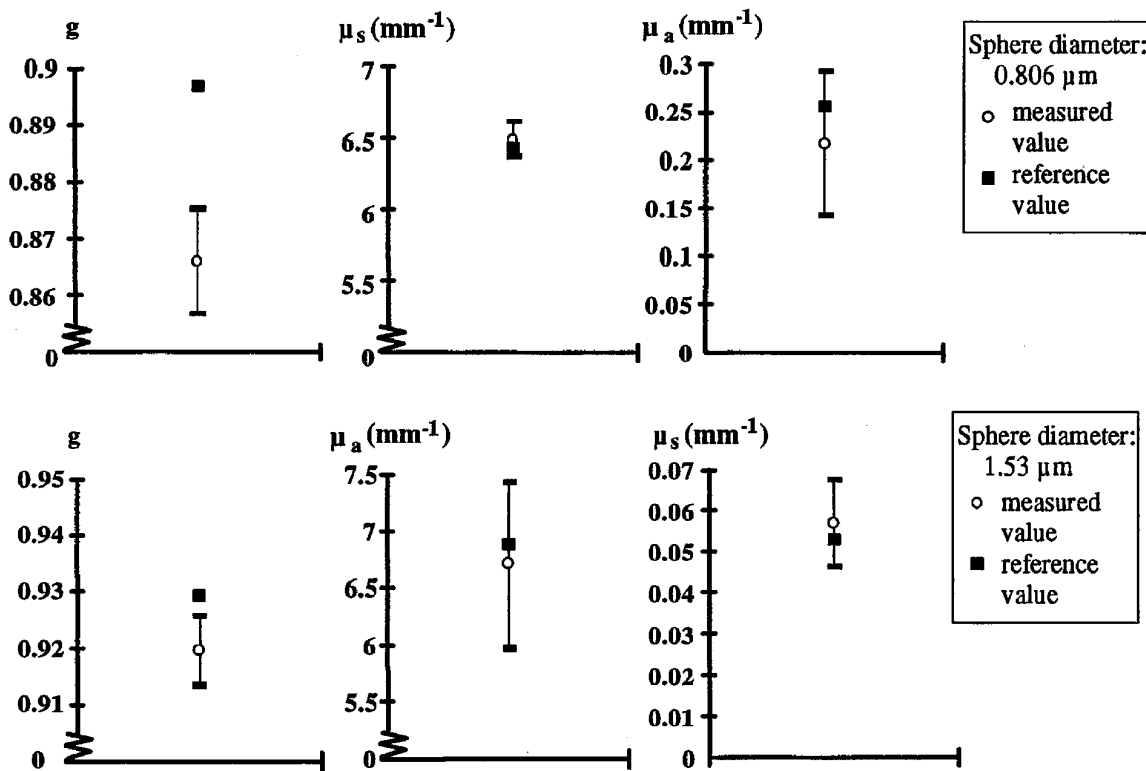Fig. 4. Optical properties of polystyrene sphere–ink suspensions at 650 nm for two different sphere diameters as measured with the integrating-sphere setup: 0.806 μm (upper plots) and 1.53 μm (lower plots) are represented by the open circles. Those results are compared with the reference values (solid squares) for g and μ_s (calculated with the Mie scattering theory) and μ_a (measured with a spectrophotometer).
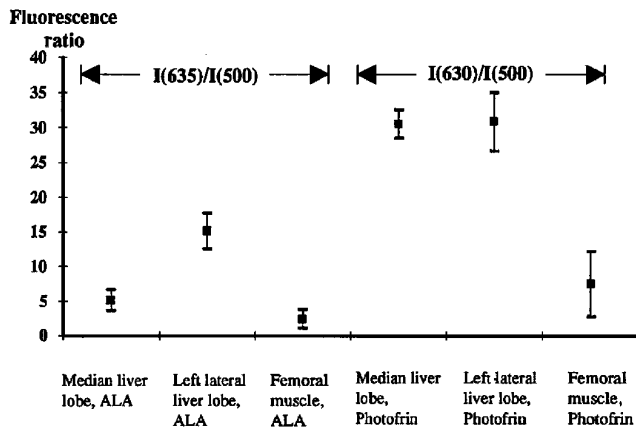
Fig. 5. Derived mean values and standard deviations of the dimensionless fluorescence ratio for the three tissue types: muscle tissue, median liver lobe, and left-lateral liver lobe. The photosensitizers used were ALA (30 mg/kg b.w.) and Photofrin (15 mg/kg b.w.).

and 30.3 for the second liver lobe. The muscle tissue from both ALA- and Photofrin-injected rats showed much lower fluorescence ratios: on average approximately 2.4 for the ALA-injected rats and 7.4 for the Photofrin-injected rats. Compared with the fluorescence ratios for the liver lobes that were treated last, the ratios for the muscle tissue were 6 (ALA-injected rats) and 4 (Photofrin-injected rats) times lower.

D. Optical-Interaction Coefficients before and after PDT

Figure 6 presents typical interaction coefficients measured on one of the nine ALA-injected rats for both treated and nontreated tissue at seven wavelengths between 500 and 800 nm. Figure 6(a) shows the optical properties of liver tissue, and Fig. 6(b) shows the coefficients for muscle tissue. The liver-tissue data shown are from a sample treated 2.5 h after the ALA injection. Similar results were obtained for samples treated 30 min after injection. The filled squares represent data from untreated tissue areas and the open circles data from treated tissue regions. At 650 nm the mean value of the g factor for all nine animals was 0.91 with a standard deviation of 0.02 for
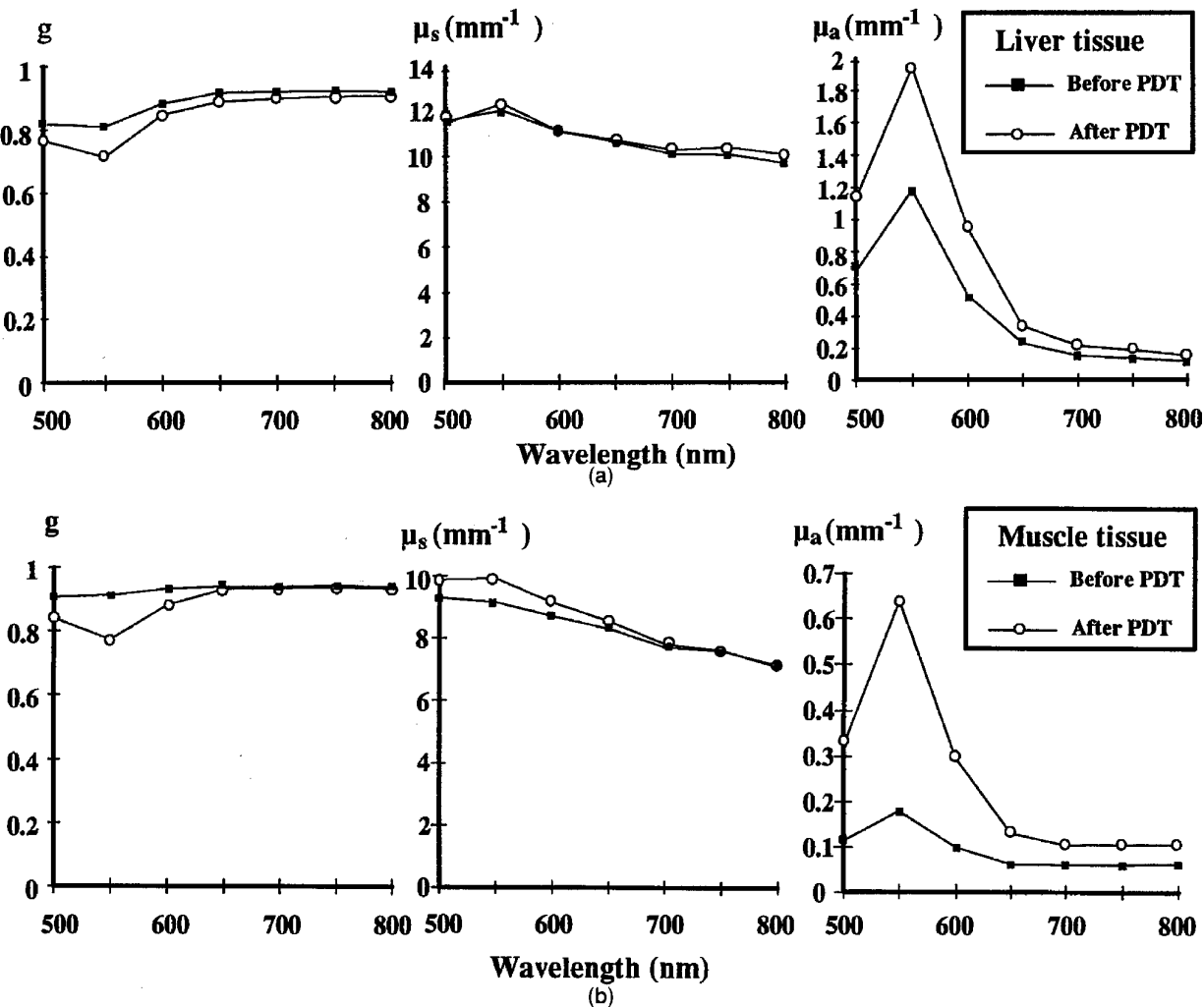

Fig. 6. The measured optical properties of PDT-treated and the surrounding nontreated tissue samples from an ALA-injected rat for (a) liver and (b) muscle.

untreated rat liver tissue; the scattering coefficient μ_s was 9.8 ± 1.2 mm^{-1}, and the absorption coefficient μ_a was 0.22 ± 0.04 mm^{-1}. For the untreated rat muscle at the same wavelength, the corresponding values were $g = 0.93 \pm 0.02$, $\mu_s = 7.9 \pm 0.9$ mm^{-1}, and $\mu_a = 0.056 \pm 0.029$ mm^{-1}. There was hardly any change in the g factor or the scattering coefficient for any of the tissues during treatment. However, the results indicate a major increase in the absorption coefficients for both tissue types. The optical properties of the tissue from the three Photofrin-injected rats in group III were similar to those of the ALA-injected rats (data not shown).

The change in optical properties during PDT was also calculated. The relative change in the anisotropy factor (in per cent) was calculated by

$$\Delta g = 100[g(\text{treated}) - g(\text{nontreated})]/g(\text{nontreated}).$$

$$(6)$$

Similar calculations were performed for the scattering and the absorption coefficients. The mean values and standard deviations of the relative changes obtained from the nine ALA-injected rats are shown in Fig. 7 as filled squares. The open circles represent the corresponding data for the three control rats, treated without any photosensitizer. None of the liver- or muscle-tissue data from the control rats (group IV) showed any significant difference in g-factor, scattering-coefficient, or absorption-coefficient values between the treated and untreated regions. This is also the case for the g factor of the tissue samples from the ALA-injected rats. The scattering coefficients of the tissue from the ALA-treated rats showed an insignificant increase from 5% to 10%, on average, for both liver and muscle tissue. However, a major change was observed in the absorption coefficients. For the liver samples treated 2.5 h after the ALA injection the absorption coefficient increased by 30% to 60% for all wavelengths and by 60–100% for the muscle tissue following the completed treatment. The results of the liver lobe treated first, i.e., treatment 30 min after the ALA injection, were approximately the same as those for the liver
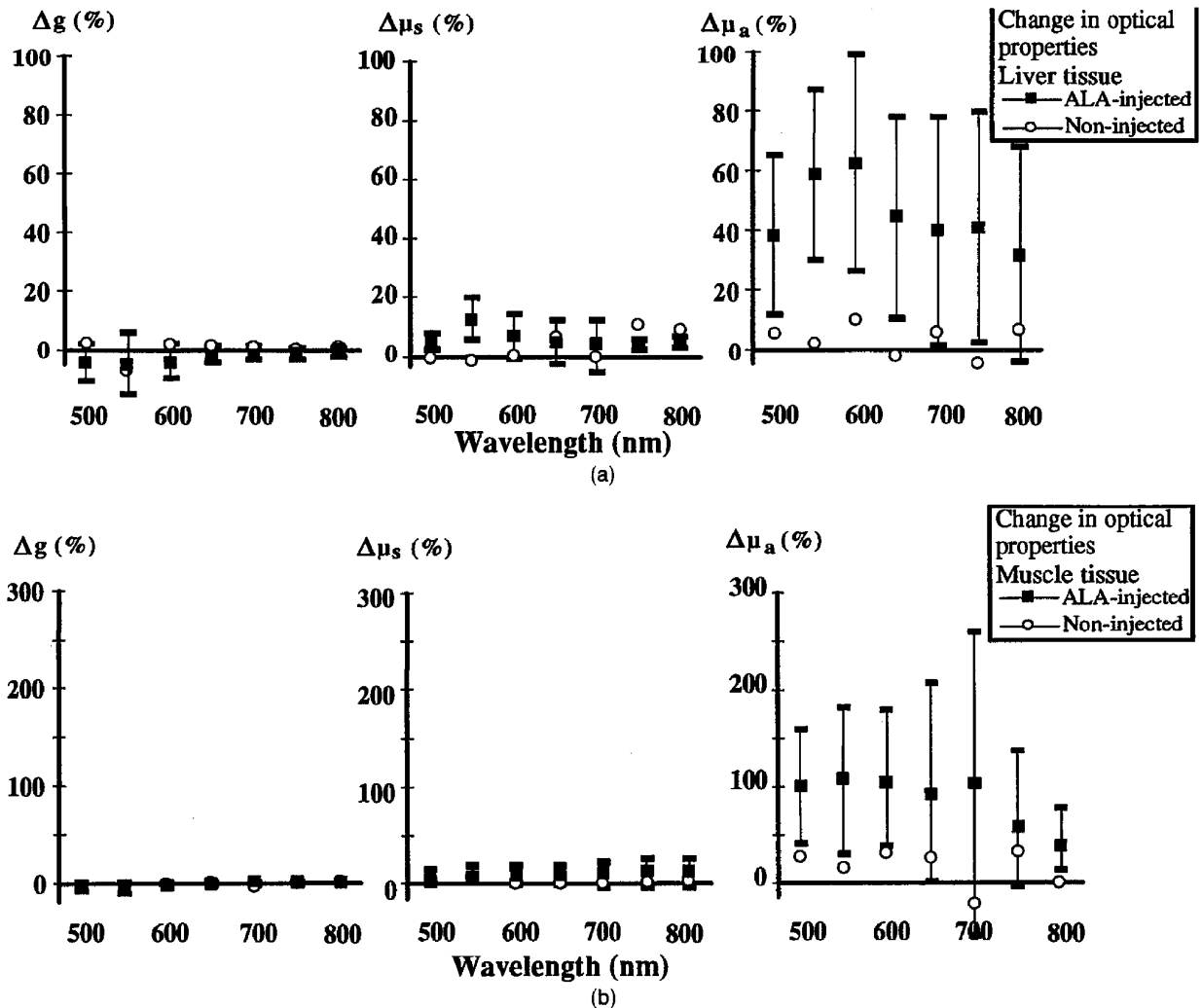

Fig. 7. Relative changes in the optical properties resulting from PDT as measured for PDT-irradiated and the surrounding nonirradiated tissues. Measurements are from ALA-injected and noninjected rats for (a) liver and (b) muscle tissue samples.

lobe treated later, i.e., no change in the g factor, an increase of 5–10% in μ_s, and an increase of 40–70% in μ_a. The changes in the optical coefficients for the samples from Photofrin-injected rats (group III) were in ranges similar to those from the ALA-injected rats. The g factor did not show any change, and μ_s was increased by 5–10% for all measured wavelengths. The absorption coefficient was, on average, increased by 30–40% for the liver tissue (both lobes) and 50–100% for the muscle tissue.

4. Discussion

Measurements of the optical properties of tissue are of major interest for most medical laser applications. This interest is demonstrated by the growing number of studies in this area. Several techniques have been developed for this purpose, each with certain applications. In this study, the optical integrating-sphere technique was chosen, as it provides a means of measurement of all three interaction coefficients from a small sample volume. For accurate values to be obtained from such measurements, a number of potential sources of error must be considered.

In the three measurements, one of the major difficulties was to measure the attenuation coefficient μ_t without any interference from scattered light. The influence of this light was greatly suppressed through the use of a highly collimated light beam and measurement of its attenuation with a small-aperture detector at a large distance from the sample. The collimated light beam was obtained when the output from the monochromator was passed through a thin optical fiber. The fiber was bent with a small curvature to ensure that all modes were properly filled. This resulted in a beam with a Gaussian profile. The light was then further spatially filtered. In this way the light intensity was considerably reduced, but a highly collimated light beam was obtained. A sensitive PMT was used as a detector to permit weak light to be detected. Recommended values of 60 cm between the sample and the detector and a 1.5-mm detector aperture were used in the narrow-beam setup.[18] The other two measurements, those of the total transmittance and the diffuse reflectance, were performed with an optical integrating sphere. In such measurements the transmitted or reflected light from the sample is reflected many times by the highly reflecting inner surface of the sphere. After a number of reflections it will reach the small detector and be registered. Approximate values of R and T can then be calculated with the simple expressions in Eqs. (2) and (3). However, errors are introduced by some simplifying assumptions made in the derivation of these equations. After the light has been transmitted through (or reflected by) the sample, the entire inner surface is considered to be highly reflective. As the small sample area (in our case 0.35% of the total sphere area) has a reduced reflectivity, this is not completely

true. A more correct analysis, without these assumptions, is described by a more generalized integrating-sphere theory.[19,20]

Not only must the potential instrumental sources of error be considered, but also the samples being investigated. With the integrating-sphere technique used in this study, one is restricted to *in vitro* measurements. For *in vitro* measurements any changes in optical properties that are due to sample preparation and degradation after resection, which is mainly caused by enzymatic processes and autolysis, must be minimized. Graaff *et al.*[21] have shown that the optical properties of human dermis measured *in vitro* differ from those measured *in vivo*. This is probably also the case for liver and muscle tissue. By simply cutting the sample without making any further sample preparation, such as freezing or grinding, and by starting the measurements only a few minutes after resection, one should be able to expect that any changes in the optical properties that are due to sample degradation should be small. In this study, our primary interest was to investigate changes in optical properties as a result of PDT and not to measure the absolute values of the optical-interaction coefficients. Thus, as both a treated and nontreated area were studied for each sample, sample degradation could not explain the observed increase in tissue absorption following PDT. Furthermore, the *in vivo* results from the experiment with the simple dosimeter are in good agreement with the results from the *in vitro* measurements.

The size of the sample is another important factor. The geometric thickness of the sample was chosen to be 1 mm to give a suitable optical thickness, τ. The optical thickness should not be too high so as not to reduce the signal-to-noise ratio, nor should it be too small to ensure a Lambertian (totally diffuse) light distribution, which is assumed for the integrating-sphere theory. An additional consideration in the choice of sample thickness is photons escaping from the sample far from the optical axis. These photons will not enter the sphere and can cause errors in the value of the absorption coefficient if they are not accounted for in the evaluation. Both Pickering *et al.*[18] and Torres *et al.*[22] point out that this fraction of lost photons is a matter of the port-to-beam-size ratio. We have checked this with the Monte Carlo simulations and found that, with a beam diameter of 5 mm and a port diameter of 25.4 mm, as we had, there is no major loss of light outside the sphere. With the optical properties of liver and muscle tissue as input parameters, 0.1–0.2% and 0.1–1%, respectively, of the reflecting and transmitting light escaped.

When using a single instead of a double integrating sphere, one has to move the sample to perform all three measurements that are needed to fully determine the optical coefficients. It is therefore important to position the sample accurately relative to the beam for all three measurements. Liver tissue was chosen because of its homogeneous structure and the

muscle tissue because of its more normal, i.e., not so high, blood perfusion. Choosing two different types of tissue also made it possible to obtain an indication of how tissue specific the change in light penetration is during PDT.

The light transport in the sample must be numerically modeled in the derivation of the optical-interaction coefficients from the μ_t, R, and T measurements. Monte Carlo simulations are well suited for this purpose, as they can be performed for any geometry and for multiple layers. Additionally, this model takes into account mismatched boundary conditions and can be adjusted to account for the side losses mentioned above.[23] The method of Monte Carlo simulations is today considered to be one of the most accurate light-transport models. The major drawback of these simulations is the considerable computing time required. To obtain a complete set of optical properties, several Monte Carlo simulations are necessary, in a so-called inverse Monte Carlo routine, to fit the measured reflectance and transmittance to the simulated values.[23] We have dealt with this by making a table of Monte Carlo-simulated data, from which the optical properties can be determined by fast spline interpolations. The disadvantage is that a new table must be constructed for each sample geometry used. This strategy initially requires much computer capacity, but, once the table has been created, the major part of the computing is done.

The calibration measurements were made with the same sample geometry and with the optical properties of the calibration solution in the same range as for the tissues studied. The results showed very good agreement between the derived optical constants and the reference values. The calibration thus confirms the negligible influence of the approximation of the sphere theory and of the lost photons described above in this particular range of optical thickness.

The optical properties of rat-liver tissue at 650 nm were determined to be

- $g = 0.91 \pm 0.02$,
- $\mu_s = 9.8 \pm 1.2$ mm^{-1},
- $\mu_a = 0.22 \pm 0.04$ mm^{-1}.

Here, the standard deviations indicate the spread in values among different animals. These can be compared with liver-tissue data published earlier by Parsa *et al.*[24] at 633 nm:

- $g = 0.95$,
- $\mu_s = 14.37$ mm^{-1},
- $\mu_a = 0.65$ mm^{-1}.

Also for comparison are liver-tissue data from van Hillegersberg *et al.*[11]:

- $g = 0.952$,
- $\mu_s = 28$ mm^{-1},
- $\mu_a = 0.38$ mm^{-1}.

The optical properties of muscle tissue are difficult to compare, as the reported results are from different types of muscle samples.[3]

When the optical properties of an untreated part of a tissue sample from groups II and III (ALA- and Photofrin-injected rats, respectively) were compared with those of a treated part of the same tissue sample, the results showed no major change in the scattering coefficient or the g factor, but there was a 30–100% increase in the absorption coefficient. Furthermore, the reference group (group IV), without any injected photosensitizers, did not show any significant change in optical coefficients. As we kept the power density at the same level, well below 100 mW/cm², for all PDT treatments, the increase in μ_a cannot be due to any laser-induced hyperthermic processes in the tissue. This proves that the observed effect is connected to the photochemical reaction in the tissue, for which a combination of photosensitizers and light is needed. Additionally, Roggan *et al.*[23] showed that tissue coagulation caused by hyperthermia results in unchanged absorption coefficients and in increased scattering coefficients—the very opposite to that observed during PDT irradiation.

Comparing the results of groups II and III, we found that the increase in μ_a was independent of whether ALA or Photofrin was used. After systemic administration of either of these drugs, the endothelial cells of the blood vessels are photosensitized. During delivery of the PDT irradiation, the blood perfusion will decrease and the vessel walls will be destroyed.[25,26] Furthermore, the change in the optical properties was the same for the two concentrations of photosensitizers present in the liver, as measured with fluorescence recordings. Although the fluorescence ratio of the liver lobe treated last, i.e., treatment 2.5 h after the injection of group II (ALA) rats, was 3 times higher than the ratio of the liver lobe treated first (treatment 30 min after the injection of ALA), no difference in the increase in μ_a between these two groups of treated liver lobes resulted. This can be explained by the fact that there was probably enough photosensitizer in the liver lobes at both times to result in the tissue damage that caused the change in absorption. The porphyrin fluorescence, evaluated as a ratio as well as on an absolute scale, was, for both drugs, considerably lower for muscle than for liver tissue. The relative change in the absorption coefficient was nearly the same in muscle as for liver tissue. Both the absorption coefficient and its PDT-related increase were, however, smaller in absolute terms than those for liver tissue. For all groups, the relative change in absorption was approximately the same for all seven wavelengths studied. This result suggests that an increased concentration of the major tissue absorber, hemoglobin, caused the elevated tissue absorption following PDT. The effect can be due to damage to the tissue microcirculation during PDT, as described in Ref. 1, which starts with microagglutination of the

blood cells and is followed by blood stasis. The blood vessels become dilated and full of red blood cells, which may lead to a more efficient attenuation of the treatment light. This phenomenon mainly causes increased absorption of the tissue, whereas the scattering is effectively unaltered. The light-penetration depth thus decreases, and the effect of the treatment becomes more superficial. As the increase in the absorption coefficient for muscle tissue is in absolute terms much smaller than for liver tissue, the reduction of the light-penetration depth is not expected to be as significant in muscle as it is in liver tissue.

The decreased light intensity measured *in vivo* with the simple optical dosimeter is in good agreement with an increased tissue absorption measured *in vitro* with the integrating-sphere technique. Results from similar *in vivo* measurements with fibers inserted into the tissue in conjunction with PDT of human skin tumors are presented in Ref. 27 and show an intensity decrease during the treatment. However, the authors[27] suggest blood coagulation around the fiber ends as a possible explanation of this decrease. The results of the integrating-sphere measurements in this study suggest an additional explanation, i.e., an increased absorption coefficient resulting from the treatment. An increase in the effective PDT light attenuation in tissue that is due to an increase in the absorption coefficient probably influences the effect of the treatment.

Two liver lobes were not immediately resected after PDT, as were the others, but were left in the rat for approximately 40 min before the integrating-sphere measurements. After resection, the optical properties were derived as for the other samples. The absorption coefficient of the treated area, in contrast to specimens immediately resected, was almost the same as, or even lower than, that for the nontreated area. As for the other samples, neither the scattering coefficient nor the g factor was significantly changed. These results indicate that the increase in the absorption coefficient occurs almost momentarily, in connection with the treatment, and is followed after a while by a decrease to its original value. One of the light-penetration measurements is in agreement with this observation, showing a slight recovery of the light intensity after 5 to 10 min. This recovery should lead to deeper light penetration and higher light intensities at distal tumor locations. Such results indicate the advantage of fractionated treatment, as suggested by others.[28,29] Berg *et al.*[28] claim better treatment results with the fractionation of light because of an increased photosensitivity of tetra(4-sulfonatophenyl)porphine (TPPS$_4$) after an initial, small light dose. The main light dose is then administered after 30–90 min. Anholt *et al.*[29] found that the photosensitizer aluminum tetrasulphonated pthalocyanine (AlPcS$_4$) did not respond as well to one exposure as to a fractionated exposure. A relocalization of the photosensitizers during a longer illumination period, reducing the treatment effect, and a different effect on the vascular system, were assumed to be the explanation. Further investigations of the effect of fractionated treatment with ALA or Photofrin as photosensitizers are suggested.

References

1. A. Castellani, G. P. Pace, and M. Concioli, "Photodynamic effect of haematoporphyrin on blood circulation," J. Pathol. Bacteriol. **86,** 99–102 (1963).
2. M. W. R. Reed, F. N. Miller, T. J. Wieman, M. T. Tseng, and C. G. Pietsch, "The effect of photodynamic therapy on the microcirculation," J. Surg. Res. **45,** 452–459 (1988).
3. W. F. Cheong, S. A. Prahl, and A. J. Welch, "A review of the optical properties of biological tissues," IEEE J. Quantum Electron. **26,** 2166–2185 (1990).
4. S. Andersson-Engels, R. Berg, and S. Svanberg, "Effects of optical constants on time-gated transillumination of tissue and tissue-like media," J. Photochem. Photobiol. **16,** 155–167 (1992).
5. M. S. Patterson, B. Chance, and B. C. Wilson, "Time resolved reflectance and transmittance for the noninvasive measurement of optical properties," Appl. Opt. **28,** 2331–2336 (1989).
6. M. S. Patterson, B. C. Wilson, and D. R. Wyman, "The propagation of optical radiation in tissue. I. Models of radiation transport and their application," Lasers Med. Sci. **6,** 155–168 (1991).
7. M. S. Patterson, B. C. Wilson, and D. R. Wyman, "The propagation of optical radiation in tissue. II. Optical properties of tissue and resulting fluence distributions," Lasers Med. Sci. **6,** 379–390 (1991).
8. P. Kubelka, "New contributions to the optics of intensely light-scattering materials. Part I.," J. Opt. Soc. Am. **38,** 448–457 (1948).
9. A. Ishimaru, "Diffusion of light in turbid material," Appl. Opt. **28,** 2210–2215 (1989).
10. S. A. Prahl, M. J. C. van Gemert, and A. J. Welch, "Determining the optical properties of turbid media by using the adding–doubling method," Appl. Opt. **32,** 559–568 (1993).
11. R. van Hillegersberg, J. W. Pickering, M. Aalders, and J. F. Beek, "Optical properties of rat liver and tumor at 633 nm and 1064 nm: Photofrin enhances scattering," Lasers Surg. Med. **13,** 31–39 (1993).
12. M. Keijzer, S. L. Jacques, S. A. Prahl, and A. J. Welch, "Light distribution in artery tissue: Monte Carlo simulations for finite-diameter laser beams," Lasers Surg. Med. **9,** 148–154 (1989).
13. S. Andersson-Engels, Å. Elner, J. Johansson, S.-E. Karlsson, L. G. Salford, L.-G. Strömblad, K. Svanberg, and S. Svanberg, "Clinical recordings of laser-induced fluorescence spectra for evaluation of tumour demarcation feasibility in selected clinical specialities," Lasers Med. Sci. **6,** 415–424 (1991).
14. L. Wang and S. L. Jacques, "Monte Carlo modeling of light transport in multi-layered tissues in standard C," rep. (Laser Biology Research Laboratory, M. D. Anderson Cancer Center, University of Texas, 1515 Holcombe Boulevard, Houston, Tex., 1992).
15. S. L. Jacques, C. A. Alter, and S. A. Prahl, "Angular dependence of He–Ne laser light scattering by human dermis," Lasers Life Sci. **1,** 309–333 (1987).

16. J. R. Zijp and J. J. ten Bosch, "Pascal program to perform Mie calculations," Opt. Eng. **32,** 1691–1695 (1993).
17. R. Graaf, J. G. Aarnoudse, J. R. Zijp, P. M. A. Sloot, F. F. M. de Mul, J. Greve, and M. H. Koelink, "Reduced light-scattering properties for mixtures of spherical particles: a simple approximation derived from Mie calculations," Appl. Opt. **31,** 1370–1376 (1992).
18. J. W. Pickering, S. A. Prahl, N. van Wieringen, J. F. Beek, H. J. C. M. Sterenborg, and M. J. C. van Gemert, "Double-integrating-sphere system for measuring the optical properties of tissue," Appl. Opt. **32,** 399–410 (1993).
19. J. W. Pickering, C. J. M. Moes, H. J. C. M. Sterenborg, S. A. Prahl, and M. J. C. van Gemert, "Two integrating spheres with an intervening scattering sample," J. Opt. Soc. Am. A **9,** 621–631 (1992).
20. D. G. Goebel, "Generalized integrating-sphere theory," Appl. Opt. **6,** 125–128 (1967).
21. R. Graaf, A. C. M. Dassel, M. H. Koelink, F. F. M. de Mul, J. G. Aarnoudse, and W. G. Zijlstra, "Optical properties of human dermis *in vitro* and *in vivo,*" Appl. Opt. **32,** 435–447 (1993).
22. J. H. Torres, A. J. Welch, I. Cilesiz, and M. Motamedi, "Tissue optical property measurements: overestimation of absorption coefficient with spectrophotometric techniques," Lasers Surg. Med. **14,** 249–257 (1994).
23. A. Roggan, H. Albrecht, K. Dörschel, O. Minet, and G. J. Müller, "Experimental setup and Monte Carlo model for the determination of optical tissue properties in the wavelength range 330–1100 nm," in *Laser Interaction with Hard and Soft Tissue II,* G. P. Delacratez, L. O. Svaasand, and R. W. Steiner, eds., Proc. Soc. Photo-Opt. Instrum. Eng. **2323,** 21–46 (1995).
24. P. Parsa, S. L. Jacques, and N. S. Nishioka, "Optical properties of rat liver between 350 and 2200 nm," Appl. Opt. **28,** 2325–2330 (1989).
25. S. Andersson-Engels, J. J. Johansson, D. Killander, E. Kjellén, M. Olivo, L. O. Svaasand, K. Svanberg, and S. Svanberg, "Photodynamic therapy alone and in conjunction with near-infrared light-induced hyperthermia in human malignant tumors: a methodological case study," in *Laser Interaction with Tissue,* M. W. Berns, ed., Proc. Soc. Photo-Opt. Instrum. Eng. **908,** 116–125 (1988).
26. W. M. Star, H. P. A. Marijnissen, A. E. van den Berg-Blok, J. A. C. Versteeg, K. A. P. Franken, and H. S. Reinhold, "Destruction of rat mammary tumor and normal tissue microcirculation by hematoporphyrin derivative photoradiation observed *in vivo* in sandwich observation chambers," Cancer Res. **46,** 2532–2540 (1986).
27. E. J. Hudson, M. R. Stringer, F. Cairnduff, D. V. Ash, and M. A. Smith, "Optical interaction coefficients of skin tumours obtained during superficial photodynamic therapy," Lasers Med. Sci. **9,** 99–103 (1994).
28. K. Berg, K. Madslien, and J. Moan, "Retention and phototoxicity of tetra(4-sulfonatophenyl)porphine in cultivated human cells. The effect of the fractionation of light," J. Photochem. Photobiol. **56,** 177–183 (1992).
29. H. Anholt and J. Moan, "Fractionated treatment of CaD2 tumors in mice sensitized with aluminium phthalocyanine tetrasulfonate," Cancer Lett. **61,** 263–267 (1991).